

REFERENCE-FREE EPI NYQUIST GHOST CORRECTION USING ANNIHILATING FILTER-BASED LOW RANK HANKEL MATRIX FOR K-SPACE INTERPOLATION

Juyoung Lee, Kyong Hwan Jin, Jong Chul Ye

Bio-Imaging and Signal Processing Lab., Dept. Bio & Brain Engineering
Korea Advanced Institute of Science & Technology (KAIST)

ABSTRACT

MR measurements from an EPI sequence produce Nyquist ghost artifacts that originate from inconsistencies between odd and even echoes. By converting the ghost correction problem to an interpolation problem from uniformly down-sampled even and odd phases, here we propose a single pass reference free ghost artifact removal algorithm. Specifically, our algorithm exploits an observation that the difference between the even and odd echoes is a Fourier transform of an underlying sparse image. Accordingly, we can construct a rank-deficient Hankel structured matrix in k-space, whose missing data can be recovered using recently proposed annihilating filter-based low rank Hankel structured matrix completion approach (ALOHA). The proposed method was applied to EPI data for both single and multi-coil acquisitions. Experimental results using in-vivo data confirmed that the proposed method can completely remove ghost artifacts successfully without any pre-scan data.

Index Terms— MRI, EPI, Nyquist ghost artifact correction, annihilating filter, structured low rank Hankel matrix completion

1. INTRODUCTION

Echo-planar imaging (EPI) acquires MR images rapidly by tracing a complete k-space in a single RF, so it is commonly used in applications that require high temporal resolution. Because of the mismatches between even and odd echoes, EPI suffers from Nyquist ghost artifacts. There have been many studies for ghost artifact corrections. These methods can be divided into two categories: navigator-based and navigator-free methods. Navigator images, which are often called as pre-scans or reference scans, are obtained without phase encoding blips. From these images, the difference between even and odd echoes can be calculated. Because it takes too much time to obtain fMRI data with a full reference scan, just two or three echoes are usually acquired in practice. However, the navigator method still has a disadvantage, because it needs extended acquisition time. On the other hand, navigator free

methods have been proposed to correct ghost artifacts without navigator scans. For example, one could correct ghost artifacts using a pulse sequence compensation, or modification [1, 2] or one could remove ghost without additional references and pulse modifications[3]. However, most of the existing reference free ghost correction methods are prone to errors and provide significantly lower performance compared to the reference-based approaches. This is why the current standard EPI ghost correction algorithms use additional reference scans.

In this paper, we proposed a novel Nyquist ghost correction method that may completely overcome the shortcomings of all the existing methods. Specifically, the proposed method does not require reference echoes but still outperforms the reference-based approach. Hence, we can safely use a conventional EPI pulse sequence without any additional pulse sequence modification. Moreover, unlike the recent parallel imaging approaches for ghost correction, our algorithm works even with a single coil measurement and it does not require any coil sensitivity map estimation or auto-calibration lines for the multi-coil acquisition.

2. SPARSIFYING PROPERTY IN EPI MODEL

An EPI sequence can be expressed as

$$S_n(k_x, k_y) = \int \int m(x, y) e^{j2\pi[\Delta f(x, y)(TE + (n-N/2)ESP)]} \cdot e^{j2\pi[\Delta f(x, y)(-1)^n (\frac{k_x}{\gamma G_x}) + k_x x + k_y y]} dx dy \quad (1)$$

where m is the image intensity and Δf is the frequency offset due to the field inhomogeneity. TE is the echo time, and ESP denotes the echo spacing. The total number of echoes is denoted by N , and n is the index of each line. G_x is a gradient for the x (readout) direction. We can notice that EPI measurements have different polarities at each even and odd line, because the $(-1)^n$ term in (1) changes its sign depending on the even and odd lines. This is why $N/2$ Nyquist ghost artifacts appear. To observe this in detail, we define the fol-

This work was supported by Korea Science and Engineering Foundation under Grant (NRF-2014R1A2A1A11052491).

lowing two sets of *virtual* k-space data:

$$S_{n,+}(k_x, k_y) = \int \int A(x, y) e^{j2\pi\Delta f(x, y) \frac{k_y}{\gamma G_x}} \cdot e^{j2\pi(k_x x + k_y y)} dx dy \quad (2)$$

$$S_{n,-}(k_x, k_y) = \int \int A(x, y) e^{-j2\pi\Delta f(x, y) \frac{k_y}{\gamma G_x}} \cdot e^{j2\pi(k_x x + k_y y)} dx dy \quad (3)$$

where

$$A(x, y) = m(x, y) e^{j2\pi\Delta f(x, y)(TE + (n-N/2)ESP)}.$$

The even or odd echo signals from the actual EPI measurement can be identified as 1/2-subsampled k-space data from $S_{n,+}(k_x, k_y)$ or $S_{n,-}(k_x, k_y)$, respectively. Therefore, by developing a high performance k-space interpolation method that can estimate the missing virtual k-space data from the actual even and odd EPI k-space data, there is chance to remove the ghost artifacts.

When two sets of *virtual* k-space data from different polarities are subtracted, the ghost generating phase term can be changed into a sine term:

$$\begin{aligned} S_{n,\Delta}(k_x, k_y) &= S_{n,+}(k_x, k_y) - S_{n,-}(k_x, k_y) \\ &= \int \int A(x, y) 2j \sin\left(2\pi\Delta f(x, y) \frac{k_x}{\gamma G_x}\right) \cdot e^{j2\pi(k_x x + k_y y)} dx dy \end{aligned} \quad (4)$$

where $S_{n,\Delta}$ is the difference between $S_{n,+}$ and $S_{n,-}$. Moreover, if the frequency offset $\Delta f(x, y)$ is sufficiently small, then

$$\sin\left(2\pi\Delta f(x, y) \frac{k_x}{\gamma G_x}\right) \simeq 2\pi\Delta f(x, y) \frac{k_x}{\gamma G_x}, \quad (5)$$

hence, we have

$$\begin{aligned} S_{n,\Delta}(k_x, k_y) &\simeq j2\pi k_x \int \int \frac{2}{\gamma G_x} A(x, y) \Delta f(x, y) \cdot e^{j2\pi(k_x x + k_y y)} dx dy \\ &= \frac{2}{\gamma G_x} \mathcal{F} \left[\frac{\partial A(x, y) \Delta f(x, y)}{\partial x} \right] \end{aligned} \quad (6)$$

where \mathcal{F} denotes the 2D Fourier transform.

Eq.(6) implies that the difference between odd and even virtual k-space data is a Fourier transform of a gradient of image multiplied by the RF offset, i.e. $\partial A(x, y) \Delta f(x, y) / \partial x$. Since $A(x, y) \Delta f(x, y)$ is relatively smooth in most of the images (which is the same assumption for total variation (TV) based modeling), it is easy to see that $\partial A(x, y) \Delta f(x, y) / \partial x$ is sparse. In fact, the sine term in (4) makes the image sparse by nulling out the signals with small argument. Therefore, our goal is to find an algorithm that exploits the sparsifying property of (4).

3. ALOHA FOR EPI GHOST CORRECTION

The sampling pattern for even and odd echoes in EPI is a uniform down-sampling pattern, so the existing compressed sensing MRI approaches [4] are difficult to use. On the other hand, a recent algorithm called annihilating filter based low rank Hankel matrix approach (ALOHA)[5] is a direct k-space interpolation approach that does not require an initial estimate. Specifically, ALOHA is based on the fundamental duality that converts a sparse signal recovery problem to a k-space interpolation problem using a low-rank interpolator. In spite of conversion to an interpolation problem, ALOHA does not lose optimality compared to the standard compressed sensing approach. Therefore, we can apply ALOHA for EPI ghost correction instead of compressed sensing.

One of the important properties of EPI that is exploited in ALOHA formulation is the *intrinsic* k-space weighting within the $S_{n,\Delta}(k_x, k_y)$. In fact, Eq. (6) implies that $S_{n,\Delta}(k_x, k_y)$ is indeed by itself a weighted k-space measurement with the weighting factor of $j2\pi k_x$, which corresponds to the spatial domain derivative along the read-out direction. Accordingly, $S_{n,\Delta}(k_x, k_y)$ represents the k-space measurement of its gradient which is usually sparse, so we can exploit the low rankness of Hankel structured matrix that is constructed by the image difference $S_{n,\Delta}(k_x, k_y)$.

According to ALOHA principle, the sparsity in the difference image implies that there exists an annihilating filter vector \mathbf{h} such that

$$\mathcal{H}(S_{n,\Delta})\mathbf{h} = (\mathcal{H}(S_{n,+}) - \mathcal{H}(S_{n,-}))\mathbf{h} = \mathbf{0} \quad (7)$$

This implies that

$$\mathcal{Y} \begin{bmatrix} \mathbf{h} \\ -\mathbf{h} \end{bmatrix} = \mathbf{0},$$

where

$$\mathcal{Y} = [\mathcal{H}(S_{n,+}) \quad \mathcal{H}(S_{n,-})] \quad (8)$$

The concatenated matrix \mathcal{Y} , which is obtained by stacking the two Hankel matrices from even and odd echoes, is low-rank. Therefore, using a low rank structured matrix completion algorithm for \mathcal{Y} , we can fill in the missing odd and even k-space lines for $S_{n,+}$ and $S_{n,-}$. Then, the final ghost-free image can be obtained as a sum of squares (SSoS) of the even and odd line image reconstructions (see Fig. 1).

In the case of multi-coil parallel imaging measurement, we can use the following parallel coil augmented matrix to fully exploit the coil diversity:

$$\tilde{\mathcal{Y}} = [\mathcal{Y}^{(1)} \quad \dots \quad \mathcal{Y}^{(r)}] \quad (9)$$

where $\mathcal{Y}^{(i)}$ denotes the even- and odd- echo concatenated Hankel matrix as in (8) for the i -th coil measurement. The optimality of constructing (9) is studied in our work [5].

ALOHA-based ghost artifact correction for single coil EPI data can be formulated by the following nuclear norm

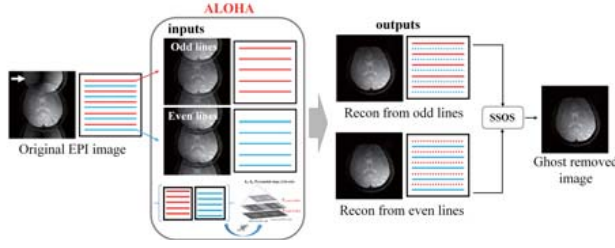


Fig. 1: ALOHA-based EPI ghost correction algorithm flow.

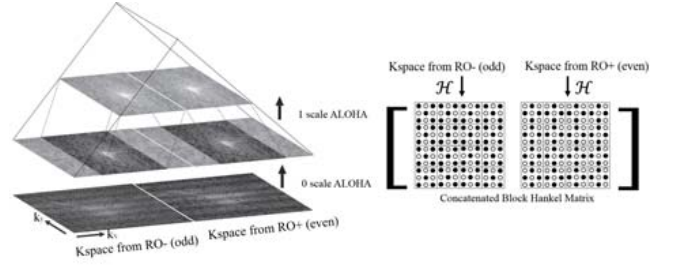


Fig. 2: Pyramidal decomposition.

minimization problem:

$$(P) \quad \min \quad \|\mathcal{H}(M_+) \mathcal{H}(M_-)\|_*$$

$$\text{subject to} \quad P_{\Omega_+}(M_+) = P_{\Omega_+}(S_{n,+})$$

$$P_{\Omega_-}(M_-) = P_{\Omega_-}(S_{n,-})$$

where $\|\cdot\|_*$ denotes a nuclear norm, and P_{Ω} is a projection operator on the sampling index set Ω , and Ω_- and Ω_+ denote the odd and even sampling index. Here, no explicit weighting is used in (P) because $S_{n,\Delta}$ has already built-in *intrinsic* weighting as described before. We used pyramidal decomposition along the readout direction as shown in Fig. 2 without using an explicit weighting. To solve this nuclear norm minimization problem, ALOHA employs a SVD-free rank minimization algorithm with an initialization from low-rank factorization (LMaFit) method. The nuclear norm minimization problem (P) can be restated as the following minimization problem under the matrix factorization constraint:

$$\min_{U,V: [\mathcal{H}(M_+) \mathcal{H}(M_-)] = UV^H} \quad \|U\|_F^2 + \|V\|_F^2$$

$$\text{subject to} \quad P_{\Omega_+}(M_+) = P_{\Omega_+}(S_{n,+})$$

$$P_{\Omega_-}(M_-) = P_{\Omega_-}(S_{n,-})$$

An associated alternating direction method of multiplier (ADMM) formulation is given by :

$$L(U, V, M_+, M_-, \Lambda) := \iota(M_+) + \iota(M_-) + \frac{1}{2}(\|U\|_F^2 + \|V\|_F^2)$$

$$+ \frac{\mu}{2} \|\mathcal{H}(M_+) \mathcal{H}(M_-) - UV^H + \Lambda\|_F^2$$

where $\iota(M_-)$ is the indicator function which has 0 value when $P_{\Omega}(M_-) = P_{\Omega}(S_{n,-})$ (similar definition of $\iota(M_+)$). This ADMM formulation is solved iteratively with update of each variable.

4. RESULTS

To test the proposed method, SE-EPI (spin-echo EPI) and GE-EPI (gradient-echo EPI) data were acquired using a Siemens 3T body scanner. The acquisition parameters for SE-EPI were TR/TE = 2270/48ms, 4 z-slice with 2mm slice thickness, field of view (FOV) of $240 \times 240\text{mm}^2$, and 128×128 matrix size with 6/8 partial Fourier sampling. The acquisition parameters for GE-EPI were TR/TE = 3000/30ms, 36 z-slice with

3mm slice thickness, and the field of view (FOV) of $240 \times 240\text{mm}^2$. The matrix size was 64×64 with full Fourier sampling of phase lines. The parameters for using the ALOHA algorithm were as follows: two levels of pyramidal decomposition along the readout direction with the LMaFit tolerance value set $(10^{-1}, 10^{-2})$ and 9×9 size annihilating filter for SE-EPI; and the LMaFit tolerance value set $(10^{-2}, 10^{-3})$ and 7×7 annihilating filter for GE-EPI. All processing of the data was done using Matlab (MathWorks, Inc.).

To compare the conventional methods and the proposed method quantitatively, the ghost-to-signal ratio (GSR) was also calculated as shown in Fig. 3. GSR is defined as the magnitude ratio between a region of interest (ROI) signal and a ghost region signal, so the performance of the correction methods can be evaluated using this value. The ghost correction method using reference data with three PE lines and the method without reference are used as conventional case. The correction method without reference based on the phase disparities between the even and odd (PDEO) sampling points by assuming that the PDEO is approximately linear along the readout direction [3]. The first row show the results of SE-EPI phantom data, the second row uses SE-EPI in vivo data, and the third row uses GE-EPI in vivo data. All data are single-coil reconstruction data. The ROI and the ghost regions are also highlighted with white boxes in Fig. 3. The upper box was for the ghost region and the lower box was for the ROI. For both spin echo and gradient echo cases, the use of a direct inverse Fourier transform resulted in the highest GSR values. Also, the GSR value of the proposed method was lower than those of the conventional methods. Especially, the conventional method without reference shows sufficiently accurate result for homogeneous phantom, but the accuracy was significantly reduced for the case of inhomogeneous objects such as in vivo human brain scan.

The functional analysis results of GE-EPI data are shown in Fig. 4. For the SPM results, multi-coil reconstruction data were used. The left side is from the ghost-corrected EPI data obtained using the conventional method with reference, and the right side is from the proposed method. Pair hand-squeezing stimulation causes motor cortex activation on both sides. The true activation sites were accurately localized by the proposed method, and the activation sensitivity increased

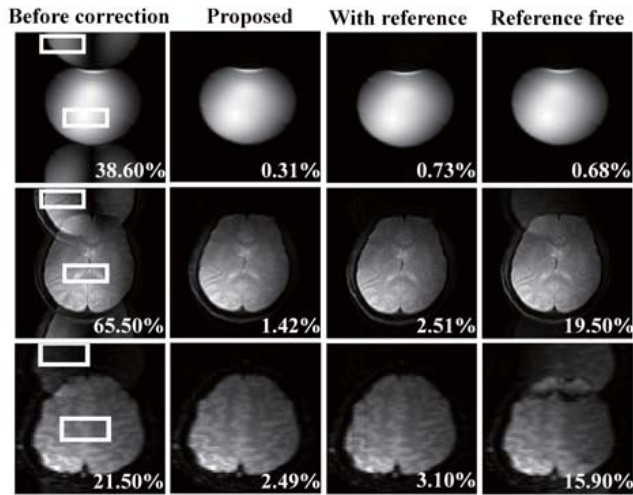


Fig. 3: Ghost correction results using the conventional methods and the proposed method. The inlayed white texts indicate the corresponding GSR values.

in the proposed method result. Meanwhile, there are some activations in other regions except motor cortex regions. The yellow highlighted slice in the SPM results is illustrated in (b) to investigate the origin of the false activation. We can see that there were signal dropouts and reconstruction artifacts (white arrow) in the results obtained using the conventional method. The conventional method can be affected by field inhomogeneity because it uses a phase map for ghost correction. Due to these artifacts, the false activation sites are shown in the corresponding slice. Also, the multi-coil ALOHA reconstruction results and the single-coil ALOHA reconstruction results are identical without signal dropout or artifacts. This implies that the removal of the signal dropout was not due to the parallel imaging; rather, it was from the annihilating filter relationship we exploited in the ALOHA algorithm.

5. CONCLUSION

We proposed a novel reference-free EPI ghost correction method using ALOHA. This method was developed based on the observation that the difference between odd and even virtual k-space data is a Fourier transform of an underlying sparse image. The ghost artifact removal problem was then converted to a missing k-space data interpolation problem that can be solved by exploiting the low rankness of the concatenated Hankel structured matrix using even and odd k-space data. To the best of our knowledge, the proposed method is the first to demonstrate complete removal of ghost artifacts without pre-scan data or modification of the pulse sequence. Moreover, because the algorithm is based on the minimal set of assumptions that are true in most of the situation, it is robust against further artifacts that can be observed in the existing prescan-based approach. We conclude that

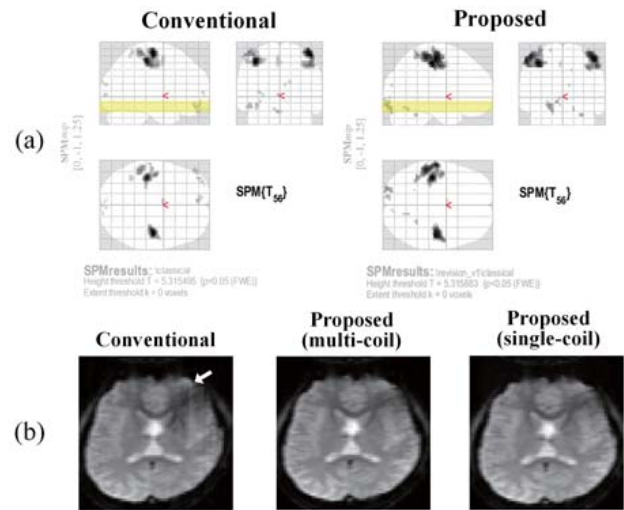


Fig. 4: Functional analysis results obtained using SPM for GE-EPI data. (a) illustrates the activation map of t -values ($p < 0.05$, corrected), and (b) shows the yellow-highlighted slice images for conventional EPI correction method, multi-coil ALOHA, and single-coil ALOHA results, respectively.

this method will be useful for many applications using EPI sequences.

6. REFERENCES

- [1] W Scott Hoge, Huan Tan, and Robert A Kraft, “Robust epi nyquist ghost elimination via spatial and temporal encoding,” *Magn. Reson. Med*, vol. 64, no. 6, pp. 1781–1791, 2010.
- [2] Benedikt A Poser, Markus Barth, Pål-Erik Goa, Weiran Deng, and V Andrew Stenger, “Single-shot echo-planar imaging with nyquist ghost compensation: Interleaved dual echo with acceleration (idea) echo-planar imaging (epi),” *Magn. Reson. Med*, vol. 69, no. 1, pp. 37–47, 2013.
- [3] Yan Zhang and Felix W Wehrli, “Reference-scan-free method for automated correction of nyquist ghost artifacts in echoplanar brain images,” *Magn. Reson. Med*, vol. 51, no. 3, pp. 621–624, 2004.
- [4] Hong Jung, Kyunghyun Sung, Krishna S Nayak, Eung Yeop Kim, and Jong Chul Ye, “k-t FOCUSS: A general compressed sensing framework for high resolution dynamic MRI,” *Magn. Reson. Med*, vol. 61, no. 1, pp. 103–116, 2009.
- [5] Kyong Hwan Jin, Dong Wook Lee, and Jong Chul Ye, “A general framework for compressed sensing and parallel mri using annihilating filter based low-rank hankel matrix,” in *arXiv 2015(1504.00532)*.